RÜHLMANN, A., KUKLA, D., SCHWAGER, P., BARTELS, K. & HUBER, R. (1973). *J. Mol. Biol.* **77**, 417–436.
SCHWAGER, P. & BARTELS, K. (1977). *The Rotation Method in Crystallography*, Ch. 10, edited by U. W. ARNDT & A. J. WONACOTT. Amsterdam, New York, Oxford: North-Holland.
SINGH, T. J., BODE, W. & HUBER, R. (1980). *Acta Cryst.* B**36**, 621–627.
STÜRZEBECHER, J., MARKWARDT, F., RICHTER, P., VOIGT, B., WAGNER, G. & WALSMANN, P. (1976). *Acta Biol. Med. Ger.* **35**, 1665–1676.
SUSSMAN, J. L., HOLBROOK, S. R., CHURCH, G. M. & KIM, S. (1977). *Acta Cryst.* A**33**, 800–804.
TAVALE, S. S., PANT, L. M. & BISWAS, A. B. (1961). *Acta Cryst.* **14**, 1281–1286.
WALTER, J. (1982). Thesis, Techn. Univ. München.
WALTER, J., STEIGEMANN, W., SINGH, T. P., BARTUNIK, H., BODE, W. & HUBER, R. (1982). *Acta Cryst.* B**38**, 1462–1472.
WARSHEL, A., LEVITT, M. & LIFSON, S. (1970). *J. Mol. Spectrosc.* **33**, 84.
WEBER, E., PAPAMOKOS, E., BODE, W., HUBER, R., KATO, I. & LASKOWSKI, M. JR (1981). *J. Mol. Biol.* **149**, 109–123.
WINKLER, F. K. & DUNITZ, J. D. (1971). *J. Mol. Biol.* **59**, 159–182.

Acta Cryst. (1983). B**39**, 490–494

The Molecular Symmetry of Histidine Decarboxylase and Prohistidine Decarboxylase by Rotation-Function Analysis

BY E. H. PARKS, K. CLINGER AND M. L. HACKERT

Department of Chemistry and Clayton Foundation Biochemical Institute, University of Texas at Austin, Austin, Texas 78712, *USA*

(*Received* 31 *August* 1982; *accepted* 19 *January* 1983)

Abstract

Several crystal forms of histidine decarboxylase (HDC) and prohistidine decarboxylase (pHDC) have been obtained, all of which contain multiple protomers per crystallographic asymmetric unit. A tetragonal crystal form of HDC and a trigonal crystal form of pHDC have been selected for further X-ray analysis. Data to resolutions of 5·6 and 5·5 Å have been collected by diffractometry for HDC and pHDC, respectively. Rotation-function studies were used to locate the non-crystallographic molecular symmetry axes. Both proteins were shown to possess 32 molecular symmetry and a cross rotation function was used to relate the two proteins in their respective unit cells. The presence of pseudo-symmetry-operator peaks complicated the analysis of the rotation-function results. In this case, the interpretation was aided by the use of cross-rotation-function results and rotation-function results based on subunit packing models.

Introduction

Histidine decarboxylase from *Lactobacillus* 30*a* is an unusual amino acid decarboxylase in that it contains a covalently bound pyruvoyl residue at the active site rather than pyridoxal-5′-phosphate (Snell, 1977; and references therein). This pyruvoyl moiety is formed from an internal serine residue during the activation of a proenzyme subunit. This proenzyme (pHDC, subunit molecular weight = 37 000) is cleaved by a seemingly intramolecular process into an α subunit ($M_r = 28\,000$) and a β subunit ($M_r = 9\,000$). It has been demonstrated that the pyruvoyl residue is required for catalysis by the formation of a Schiff-base intermediate with both histidine and histamine in a similar manner to that of pyridoxal-phosphate-dependent enzymes.

A mutant of *Lactobacillus* 30*a* was found which possessed an inactive form of histidine decarboxylase which was very slowly converted to the active histidine decarboxylase (HDC). It has recently been shown that the proenzyme (pHDC) has six associated subunits, $(\pi)_6$, whereas the native enzyme has an $(\alpha\beta)_6$ subunit stoichiometry, both forms having a molecular weight of 208 000 (Hackert, Meador, Oliver, Salmon, Recsei & Snell, 1981).

Histidine decarboxylase has been crystallized in several distinct forms, two of which have been selected for further crystallographic investigations. HDC crystallizes in a tetragonal space group ($I4_122$; $a = b = 222$, $c = 107$ Å). The unit cell contains eight molecules which occupy the 16 general positions of the unit cell. This implies that the HDC molecule has at least twofold molecular symmetry. Mutant pHDC crystallizes in a trigonal space group ($P321$; $a = b = 100$, $c = 164{\cdot}5$ Å). In this system the unit cell contains only two molecules which are positioned on the two internal

0108-7681/83/040490-05$01.50 © 1983 International Union of Crystallography

threefold symmetry axes. In other words, pHDC must have threefold molecular symmetry.

Native data sets of both HDC and pHDC have been collected and subjected to rotation-function analysis. The results reported here confirm earlier studies that implied that both forms of the enzyme have 32 molecular point-group symmetry. These results have been used to locate the relative orientations of these molecules in their respective unit cells which will be of aid in solving heavy-atom derivatives, in phase refinement *via* density averaging, and in later comparison of the proenzyme and active enzyme structures.

The analysis of these rotation-function results required the assignment of the various peaks as particle peaks, packing peaks, or pseudo-symmetry peaks. To aid in the proper interpretation of these rotation-function results, a cross rotation function between pHDC and HDC was also computed. The final interpretation was verified by comparing the experimental results with rotation-function results of models based on the implied subunit arrangements. It is anticipated that the approach used in these studies will be generally applicable for many other high-symmetry systems.

Experimental

HDC and pHDC were purified as described previously (Chang & Snell, 1968; Rescei & Snell, 1973). Crystals were grown as reported earlier (Hackert *et al.*, 1981). Data were collected to 5·6 Å for HDC and 5·5 Å resolution for pHDC on an automated four-circle diffractometer with Cu $K\alpha$ radiation using the ω-scan technique. Intensities were corrected for absorption, decay, Lorentz and polarization effects.

Rotation-function analyses were performed with a computer program based upon Tanaka's (1977) modification of the fast-rotation function (Crowther, 1972). A spherical polar coordinate system is used to define the rotation axis. Thus a search of $\chi = 120°$ will locate the threefold symmetry axes and a search of $\chi = 180°$ will locate the twofold symmetry axes. Model rotation-function studies were used to verify the interpretations of the rotation-function results. Model protein subunits for HDC were represented as spheres of uniform density. A protein fragment was used in modelling the subunits of pHDC to reduce the symmetry of the resulting model transform.

Rotation-function results

There are three types of peaks which may arise in a rotation-function search. The first type, referred to as a particle peak, is due to the presence of molecular symmetry within the particle. The second type, referred to as a packing peak, is due to the packing of the particle into the space-group lattice. The last type, referred to as a pseudo-symmetry operator or 'Klug' peak, is a consequence of the non-crystallographic symmetry elements relating the self-vector sets of the individual molecules (Lentz & Strandberg, 1974; Johnson, Argos & Rossmann, 1975). All three types of peaks have been identified in these rotation-function results.

(1) *HDC*

Figs. 1(*a*), 1(*b*), and 1(*c*) show the rotation-function sections for $\chi = 90$, 120 and 180° respectively. In Fig. 1(*a*) two types of fourfold axes are found. The first, at $\psi = 0°$, is a true packing peak with a relative height of 50 corresponding to the crystallographic fourfold screw operator. The second at $\psi = 90°$, $\varphi = 45$ and 135°, with a relative height of 44, has been assigned as a non-crystallographic and non-molecular pseudo-symmetry operator or 'Klug' peak.

In Fig. 1(*b*) only one type of threefold axis is found. This occurs at $\psi = 55°$ and $\varphi = 0$, 90, 180, and 270°. This peak is a particle peak with a relative height of 44.

Fig. 1(*c*) is somewhat more complex. The peaks at $\psi = 0°$ and at $\psi = 90°$; $\varphi = 45$ and 135° are pure packing peaks with a relative height of 50. The peaks at $\psi = 90°$; $\varphi = 0$ and 90° are particle peaks coincident with packing peaks with a relative height of 50. The last type of twofold peak is a pure particle peak with a relative height of 44. It is found at $\psi = 45°$; $\varphi = 45$, 135, 225,

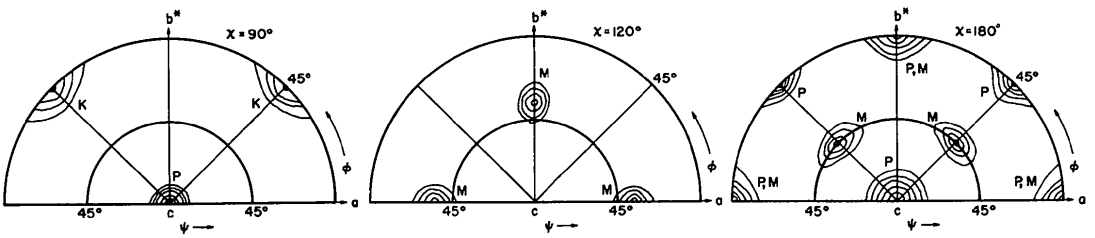

Fig. 1(*a*), (*b*), (*c*): polar projections along the *c* axis of the rotation function for $\chi = 90$, 120, and 180° (*M* particle peak, *P* packing peak, *K* 'Klug' peak). Contours are at every rise of ten in relative height. Background levels are arbitrarily taken as below 10.

and 315° and corresponds to the molecular twofold axes which are threefold-related to the crystallographic and molecular twofold axis.

This combination of crystallographic and molecular symmetry axes depicted in Fig. 1 corresponds to a pseudo-octahedral (432) symmetry system.

(2) *pHDC*

In the pHDC system the rotation function was used to verify the presence of the molecular twofold axes and to determine whether or not these were aligned with the crystallographic twofold axes. In Fig. 2 a plot of R *vs* φ is shown for $\chi = 180°$ and $\psi = 90°$. A small peak at $\varphi = 20°$ suggested the presence of a non-crystallographic twofold molecular symmetry axis.

(3) *pHDC vs HDC*

A cross rotation function was calculated for pHDC *vs* HDC to confirm the above interpretation. There are two sets of prominent peaks in the map. The rotation matrices corresponding to both sets of peaks orient the crystallographic threefold axis in the pHDC system at $\psi = 55°$ and $\varphi = 0°$ in the HDC system. This is in agreement with the interpretation of the HDC rotation-function results presented above. The inverse of the matrix corresponding to the set with the larger peaks orients the crystallographic twofold axes in the HDC system at $\psi = 90°$, $\varphi = 22°$ in the pHDC system, in agreement with the weak twofold peak observed with the pHDC system (Fig. 2). The inverse of the matrix corresponding to the second set of somewhat smaller peaks yielded a rotation matrix which placed this twofold axis at $\psi = 90°$ and $\varphi = 60°$ or aligned with the crystallographic axes in the pHDC system. These results are presented in Fig. 3(*a*) where the *ab* plane of the pHDC system is superimposed on the HDC system such that the *a* and *b** axes are aligned.

From this figure it is obvious that there are several different rotations (θ_1) about *c* which will align the molecular twofold axes in the HDC system. A second rotation (θ_2) is then required to align the crystallo-

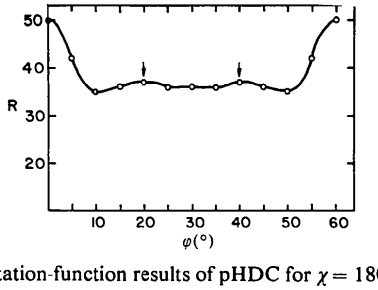

Fig. 2. Rotation-function results of pHDC for $\chi = 180°$, $\psi = 90°$.

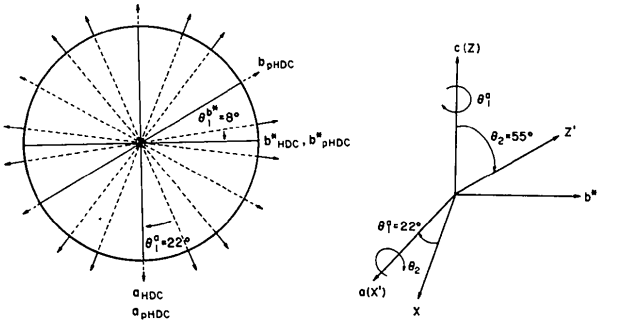

Fig. 3. (*a*) The *ab* plane of the pHDC system superimposed on the *ab* plane of the HDC system such that the *a* and *b** axes are aligned. The two sets of molecular twofold axes in the pHDC system are indicated with arrows. Best solution (→): $\theta_1^a = (n60° + 22°)$ where $n = 0, 1, 2, 3, 4, 5$; $\theta_1^b = (n60° + 8°)$. Second-best solution (– – – →): $\theta_1^a = n60°$; $\theta_1^b = (n60° + 30°)$. (*b*) The rotation of pHDC into HDC can be accomplished by a rotation of θ_1^a (or θ_1^{b*}) about z followed by a rotation of θ_2 about x'. x and z correspond to the molecular twofold and threefold axes in the pHDC system while x' and z' correspond to these same axes in the HDC system. x' will be aligned along *a* or *b** of the HDC system. $\theta_2 = 55, 125, 235, 305°$.

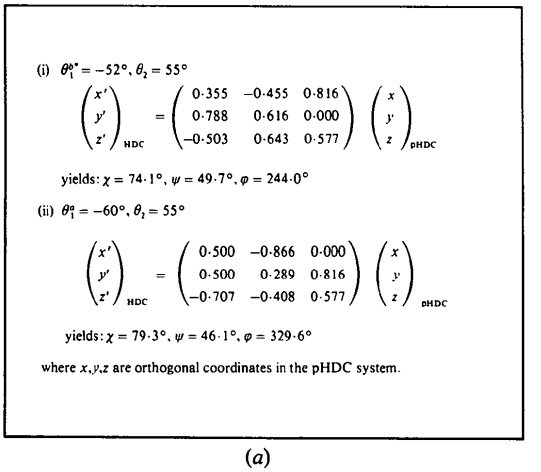

(*a*)

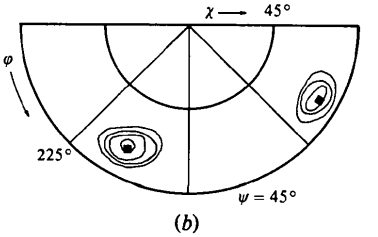

(*b*)

Fig. 4. (*a*) An example of two rotation matrices and χ, ψ and φ values obtained from the predicted rotation angles θ_1 and θ_2. Two sets of θ_1 values are predicted: the first corresponds to the weak twofold peak observed with the pHDC system, the second corresponds to the molecular twofold axis being aligned with the crystallographic pHDC twofold axes. (*b*) The $\psi = 45°$ section (χ: 0 → 90°; φ: 180 → 360°) for the pHDC *vs* HDC cross rotation function. Contours are at every rise of ten relative height. Background levels are arbitrarily taken as below 50. ■ Predicted peak positions [see (*a*)].

graphic threefold axes of the two systems as illustrated in Fig. 3(*b*). The corresponding rotation matrix can be calculated from the rotation angles θ_1 and θ_2. From this matrix the values of χ, ψ, and φ for the equivalent rotation can be obtained (*International Tables for X-ray Crystallography*, 1972; where $\alpha = \chi$, $l_1 = -\cos\varphi\sin\psi$, $l_2 = -\sin\varphi\sin\psi$ and $l_3 = \cos\psi$).

As a check of the cross-rotation-function results several matrices, and their corresponding χ, ψ and φ values, were calculated from the predicted values of θ_1 and θ_2 and then compared to the actual cross-rotation-function output. An example of this process is shown in Fig. 4.

As can be seen, the experimental peaks are found very close to the predicted positions. These peak heights are typical. The cross-rotation peaks corresponding to the molecular twofold axis positioned 22° from the crystallographic twofold axis in the pHDC system have peak heights ranging from 82 to 93. The corresponding peaks indicating a molecular twofold axis parallel with the crystallographic twofold axis have peak heights ranging from 73 to 80. All peaks greater than 70 correspond to one of these two solutions.

(4) *Model structures*

Model structures representing the subunit packing for both HDC and pHDC crystals were constructed to confirm the interpretations of the rotation-function results. The HDC model protein correctly predicted all particle, packing, and 'Klug' peaks reported above for the actual HDC rotation-function results.

Several pHDC models were constructed representing various molecular conformations. A model containing a twofold axis at $\psi = 90°$, $\varphi = 22°$ with subunits arranged in an eclipsed manner yielded peaks for $\chi = 180°$ at $\psi = 90°$, and $\varphi = 20$ and 40° which were well above background. The corresponding model in the staggered conformation produced peaks like those found in the eclipsed model, but with a much higher background similar to that found in the rotation-function results of pHDC.

Eclipsed and staggered models containing molecular twofold axes parallel to the crystallographic twofold axes also were constructed. Neither model exhibited a rotation-function peak at $\chi = 180°$, $\psi = 90°$, and $\varphi = 20°$. Since the models with the molecular twofold axes aligned along the crystallographic axes showed no peak at $\psi = 90°$ and $\varphi = 20°$ and could not account for the largest peaks in the pHDC–HDC cross-rotation-function results, they were discounted. Therefore, the molecular twofold axis was assigned to $\psi = 90°$ and $\varphi = 22°$. Furthermore, these rotation results imply that the pHDC molecule has a staggered conformation due to the similarity of the model rotation results to those of pHDC.

Discussion

Bacterial amino acid decarboxylases have been found to be large multi-subunit proteins (Boeker & Snell, 1972). High molecular symmetry may be present in these proteins which could be utilized in solving the structures of many of these enzymes. In this study, the molecular symmetries of both HDC and pHDC were determined. Both proteins exhibit 32 molecular symmetry, with the $(\alpha\beta)_6$ configuration of HDC apparently resulting from a dimerization of $(\alpha\beta)_3$ particles. The $(\alpha\beta)_3$ particles are observed only under conditions of low ionic strength and high pH (7·0 *vs* 4·8; Hackert *et al.*, 1981).

Similarly, pHDC has two $(\pi)_3$ trimers related by a molecular twofold axis to form a $(\pi)_6$ molecule (Hackert *et al.*, 1981). Another histidine decarboxylase isolated from *Micrococcus* (Prozorovski & Jornvall, 1974; Gonchar, Katsnel'son, L'vov, Semina & Feigin, 1977) possesses only threefold molecular symmetry. It consists of α and β subunits approximately the same size as the chains of HDC from *Lactobacillus* arranged to form a stable $(\alpha\beta)_3$ molecule. In contrast, mammalian histidine decarboxylase (a pyridoxal-phosphate-requiring enzyme) apparently is composed only of two non-identical subunits with molecular weights 145 000 and 66 000 respectively (Tran & Snyder, 1981).

Hackert *et al.* (1981) noted that in the *Lactobacillus* HDC system the *h*0*l* zone exhibited pseudo sixfold symmetry. It was initially thought that this implied that the molecular threefold axes of symmetry were parallel with the crystallographic *a* and *b* axes of the tetragonal cell. It is now apparent that those intensity spikes located 55° from the crystallographic *c* axis corres-

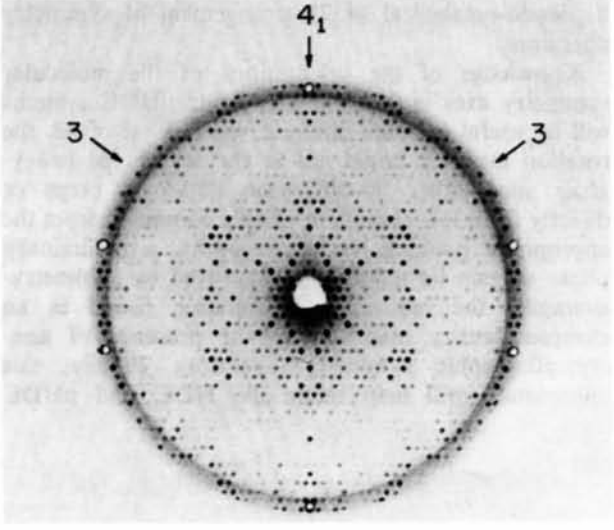

Fig. 5. Precession photograph of the *h*0*l* zone for HDC ($\mu = 10°$). The strong intensity spikes corresponding to the fourfold crystallographic axis and the threefold molecular axes are identified.

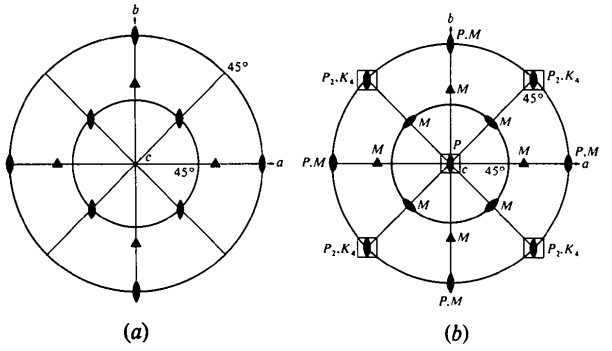

Fig. 6. (*a*) Polar projection viewed down the *c* axis of the HDC unit cell. The locations of all molecular symmetry operators are shown for HDC molecules with molecular 32 symmetry. The threefold axes of these molecules are inclined 55° from the *c* axis. (*b*) The observed polar projection down the *c* axis showing the locations and assignments of all of the symmetry operators for the HDC unit cell. (*M* molecular symmetry operator, *P* crystallographic symmetry operator, and *K* non-crystallographic and non-molecular pseudo-symmetry operator.)

pond to the projection of the molecular threefold axes of symmetry. This is illustrated in Fig. 5. Such radial spikes are often associated with molecular symmetry axes.

The orientations of the molecular symmetry elements in the unit cell of HDC are plotted in Fig. 6(*a*). The positions of the other symmetry operators also may be identified in the diagram. For example, it is obvious that the four threefold axes at $\psi = 55°$ are related by a fourfold rotation axis. Those symmetry axes which relate various molecular symmetry elements give rise to packing peaks (*P*) or 'Klug' peaks (*K*), depending upon whether or not they correspond to equivalent crystallographic axes. The results depicted in Fig. 6(*b*) constitute a pseudo-octahedral (432) arrangement of symmetry operators.

Knowledge of the orientations of the molecular symmetry axes in both the HDC and pHDC systems will be useful in three different ways. First of all, the rotation matrices could aid in the search for heavy-atom sites either in difference Patterson maps or directly from low-resolution phases computed from the appropriate packing model. Secondly, a preliminary phase set can be refined and improved by symmetry-averaging the redundant information found in an electron density map due to the presence of non-crystallographic symmetry operators. Finally, this information will help relate the HDC and pHDC systems to each other. This relationship will be useful in studying the structural changes that occur during activation.

In summary, both HDC and pHDC have been shown to possess 32 molecular symmetry. The analysis of these rotation results was complicated by the presence of pseudo-symmetry or 'Klug' peaks. It was found that proper assignment of molecular symmetry elements was greatly aided by analysis of a cross rotation function which was also used to relate the two molecules in their respective unit cells. These interpretations were confirmed by comparing the experimental rotation-function results with the results obtained from the rotation-function analysis of the implied subunit packing models similar to the approach used in the analysis of southern bean mosaic virus (Johnson *et al.*, 1975). It is anticipated that these techniques will be generally applicable to other high-molecular-symmetry systems.

We wish to acknowledge the collaboration of Drs Paul Recsei and Esmond Snell who supplied the protein for these studies. Also, we wish to thank Dr Stephen Ernst and Fred Hoffmann for their expert technical assistance and Liz Carrion for preparing the manuscript. This work was supported in part by grants (GM 2306 and GM 30105) from the United States Public Health Service.

References

BOEKER, E. A. & SNELL, E. E. (1972). *The Enzymes*, Vol. IV, edited by P. D. BOYER, 3rd ed., pp. 217–253. New York: Academic Press.

CHANG, G. W. & SNELL, E. E. (1968). *Biochemistry*, **7**, 2012–2020.

CROWTHER, R. A. (1972). *The Molecular Replacement Method*, edited by M. G. ROSSMANN, pp. 173–183. New York: Gordon and Breach.

GONCHAR, N. A., KATSNEL'SON, A. A., L'VOV, YU. M., SEMINA, L. A. & FEIGIN, L. A. (1977). *Biophysics (USSR)*, **22**, 829–834.

HACKERT, M. L., MEADOR, W. E., OLIVER, R. M., SALMON, J. B., RECSEI, P. A. & SNELL, E. E. (1981). *J. Biol. Chem.* **256**, 687–690.

International Tables for X-ray Crystallography (1972). Vol. II, 3rd ed., p. 63. Birmingham: Kynoch Press.

JOHNSON, J. E., ARGOS, P. & ROSSMANN, M. G. (1975). *Acta Cryst.* B**31**, 2577–2583.

LENTZ, P. J. & STRANDBERG, B. (1974). *Acta Cryst.* A**30**, 552–559.

PROZOROVSKI, V. & JORNVALL, H. (1974). *Eur. J. Biochem.* **42**, 405–409.

RECSEI, P. A. & SNELL, E. E. (1973). *Biochemistry*, **12**, 365–371.

SNELL, E. E. (1977). *Trends Biochem. Sci.* **2**, 131–135.

TANAKA, N. (1977). *Acta Cryst.* A**33**, 191–193.

TRAN, V. T. & SNYDER, S. H. (1981). *J. Biol. Chem.* **256**, 680–686.